Electronic Supplementary Material (ESI)

$La_3B_{14}^-$: An Inverse Triple-Decker Lanthanide Boron Cluster

Teng-Teng Chen,‡[a] Wan-Lu Li,‡[b] Wei-Jia Chen,[a] Jun Li*[bc] and Lai-Sheng Wang*[a]

[a] *Department of Chemistry, Brown University, Providence, RI 02912 USA.*

Email: Lai-Sheng_Wang@brown.edu

[b] *Department of Chemistry and Key Laboratory of Organic Optoelectronics & Molecular Engineering of Ministry of Education, Tsinghua University, Beijing 100084 China.*

Email: junli@tsinghua.edu.cn

[c] *Department of Chemistry, Southern University of Science and Technology, Shenzhen, Guangdong 518055 (China).*

Table of Contents

Experimental and Computational Details

Photoelectron spectroscopy. The experiment was performed using a magnetic-bottle PES apparatus equipped with a laser vaporization supersonic cluster source, details of which have been published elsewhere.[1, 2] Briefly, the $La_3B_{14}^-$ cluster was produced by laser ablation of a La/^{11}B disc target using 532 nm from the second harmonic of a Nd:YAG laser. The La/^{11}B composite target (5/2 mass ratio) was prepared by mixing a La metal powder (Alfa Aesar, -40 mesh, 99.7% purity) with a ^{11}B-enriched powder (Alfa Aesar, 96% ^{11}B-enriched, -100 mesh, 99.9% metal basis) inside a glove box and cold-pressed into a 12 mm diameter round disc target. The nascent clusters were entrained in a helium carrier gas containing 5% Ar and underwent a supersonic expansion. Negatively charged clusters were extracted from the collimated cluster beam perpendicularly and then analyzed by a time-of-flight mass spectrometer. The $La_3B_{14}^-$ cluster of interest was mass-selected and decelerated before being photodetached by the 193 nm radiation (6.424 eV) from an ArF excimer laser. The emitted photoelectrons were collected and analyzed by a magnetic-bottle electron analyzer. The energy resolution of the apparatus was about 2.5 %, that is, ~ 25 meV for 1 eV electrons.

Computational methods. Global minimum structure searches of $La_3B_{14}^-$ were performed using the TGMin 2.0 package,[3, 4] with the initial seeds being constructed manually. The PBE density functional[5] and Slater-type basis sets of triple-ζ plus one polarization function[6] were used in the calculations. The scalar-relativistic effect was taken into account by the ZORA approximation[7] from the ADF 2016.101 package.[8] The frozen core approximation was applied to the inner cores of [$1s^2$-$4d^{10}$] for La and [$1s^2$] for B. The remaining valence electrons were treated variationally during the SCF procedure. Relative energies of low-lying isomers within 54 kcal/mol of the global minimum were further evaluated at the level of PBE0/TZP.[9] The first vertical detachment energy (VDE) was computed from the difference of energy between the neutral and anion at the optimized anion geometry. Higher VDEs were computed using the ΔSCF-TDDFT method as employed previously.[10] The SAOP model was used here in the TDDFT calculations for better describing the long-range interactions of excited states.[11] Chemical bonding analyses were done using the AdNDP method[12] with the density matrix generated from the PBE0 density functional and visualized by the VMD package.[13]

References

1. L. S. Wang, *Int. Rev. Phys. Chem.*, 2016, **35**, 69-142.
2. L. S. Wang, H. S. Cheng and J. Fan, *J. Chem. Phys.*, 1995, **102**, 9480-9493.
3. Y. F. Zhao, X. Chen and J. Li, *Nano Res.*, 2017, **10**, 3407-3420.
4. X. Chen, Y. F. Zhao, Y. Y. Zhang and J. Li, *J. Comput. Chem.*, 2019, **40**, 1105-1112.
5. J. P. Perdew, K. Burke and M. Ernzerhof, *Phys. Rev. Lett*, 1996, **77**, 3865-3868.
6. ADF, 2016.101, SCM, Theoretical Chemistry, Vrijie Universiteit, Amsterdam, The Netherlands, (http://www.scm.com).
7. E. Van Lenthe and E. J. Baerends, *J. Comput. Chem.*, 2003, **24**, 1142-1156.
8. E. v. Lenthe, E.-J. Baerends and J. G. Snijders, *J. Chem. Phys.*, 1993, **99**, 4597-4610.
9. C. Adamo and V. Barone, *J. Chem. Phys.*, 1999, **110**, 6158-6170.
10. J. Li, X. Li, H. J. Zhai and L. S. Wang, *Science*, 2003, **299**, 864-867.
11. O. V. Gritsenko, P. R. T. Schipper and E. J. Baerends, *Chem. Phys. Lett.*, 1999, **302**, 199-207.
12. D. Y. Zubarev and A. I. Boldyrev, *Phys. Chem. Chem. Phys.*, 2008, **10**, 5207-5217.
13. W. Humphrey, A. Dalke and K. Schulten, *J. Mol. Graph.*, 1996, **14**, 33-38.

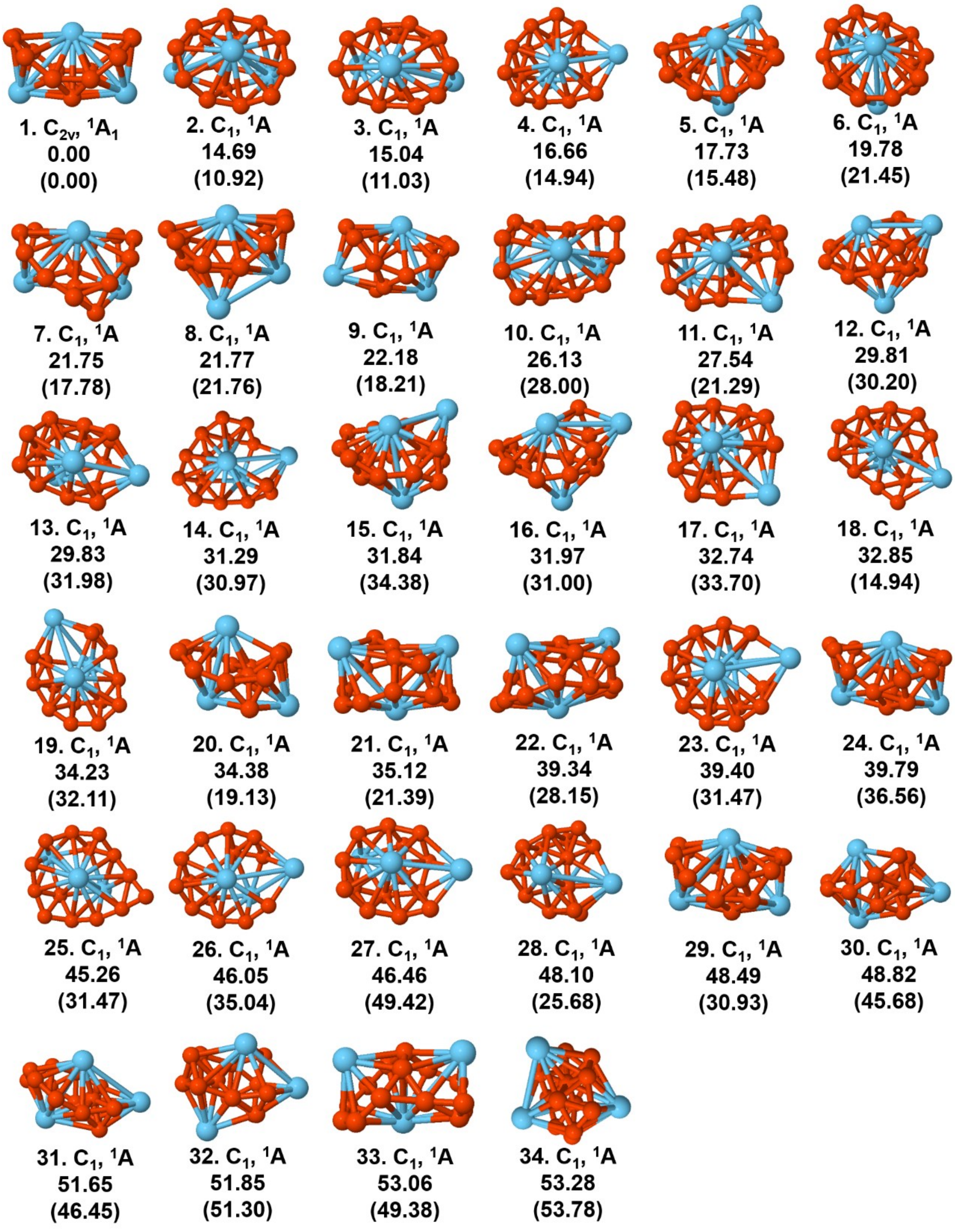

Figure S1. Relative energies in kcal/mol of the low-lying isomers of $La_3B_{14}^-$ within 54 kcal/mol of the global minimum at PBE/TZP and PBE0/TZP levels in brackets.

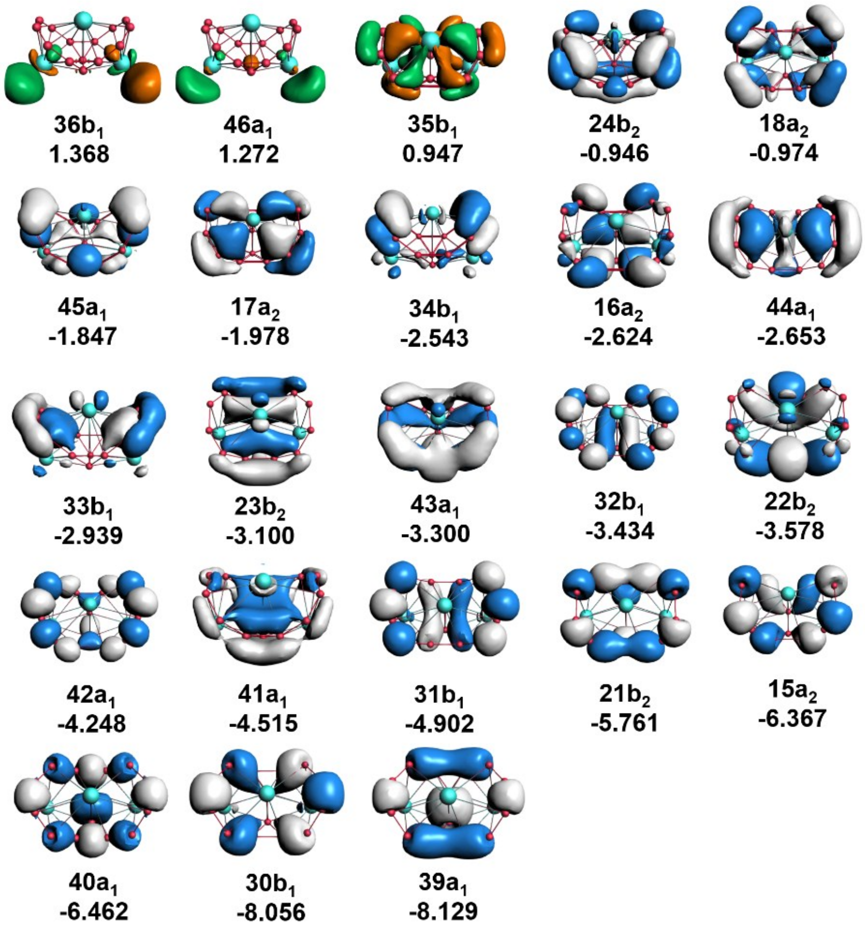

Figure S2. Frontier canonical Kohn-Sham molecular orbitals and the corresponding energies of $La_3B_{14}^-$ at the PBE0/TZP level of theory, where $24b_2$ is the HOMO and $35b_1$ is the LUMO.

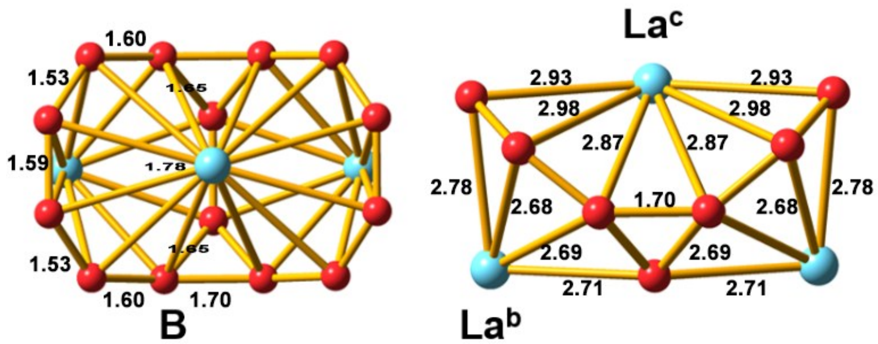

Figure S3. Bond lengths (in Å) of the titled inverse triple-decker global minimum of $La_3B_{14}^-$ at the PBE0/TZP level of theory.

Table S1. Experimental VDEs compared with theoretical VDEs, and the corresponding electronic states and configurations of the global minimum of $La_3B_{14}^-$ using the ΔSCF-TDDFT method. The bold-face indicates the primary orbitals from which an electron is detached.

	VDE (Exp)	Final State Symmetry and Electron Configuration	VDE (Theo)
X	2.25(2)	$^2B_2$, $\{\ldots 15a_2^2 21b_2^2 31b_1^2 41a_1^2 42a_1^2 22b_2^2 32b_1^2 43a_1^2 23b_2^2 33b_1^2 44a_1^2 16a_2^2 34b_1^2 17a_2^2 45a_1^2 18a_2^2 \mathbf{24b_2^1}\}$	2.18
		$^2A_2$, $\{\ldots 15a_2^2 21b_2^2 31b_1^2 41a_1^2 42a_1^2 22b_2^2 32b_1^2 43a_1^2 23b_2^2 33b_1^2 44a_1^2 16a_2^2 34b_1^2 17a_2^2 45a_1^2 \mathbf{18a_2^1} 24b_2^2\}$	2.36
A	3.15(3)	$^2A_1$, $\{\ldots 15a_2^2 21b_2^2 31b_1^2 41a_1^2 42a_1^2 22b_2^2 32b_1^2 43a_1^2 23b_2^2 33b_1^2 44a_1^2 16a_2^2 34b_1^2 17a_2^2 \mathbf{45a_1^1} 18a_2^2 24b_2^2\}$	3.05
		$^2A_2$, $\{\ldots 15a_2^2 21b_2^2 31b_1^2 41a_1^2 42a_1^2 22b_2^2 32b_1^2 43a_1^2 23b_2^2 33b_1^2 44a_1^2 16a_2^2 34b_1^2 \mathbf{17a_2^1} 45a_1^2 18a_2^2 24b_2^2\}$	3.17
B	3.71(7)	$^2B_1$, $\{\ldots 15a_2^2 21b_2^2 31b_1^2 41a_1^2 42a_1^2 22b_2^2 32b_1^2 43a_1^2 23b_2^2 33b_1^2 44a_1^2 16a_2^2 \mathbf{34b_1^1} 17a_2^2 45a_1^2 18a_2^2 24b_2^2\}$	3.58
		$^2A_2$, $\{\ldots 15a_2^2 21b_2^2 31b_1^2 41a_1^2 42a_1^2 22b_2^2 32b_1^2 43a_1^2 23b_2^2 33b_1^2 44a_1^2 \mathbf{16a_2^1} 34b_1^2 17a_2^2 45a_1^2 18a_2^2 24b_2^2\}$	3.69
		$^2A_1$, $\{\ldots 15a_2^2 21b_2^2 31b_1^2 41a_1^2 42a_1^2 22b_2^2 32b_1^2 43a_1^2 23b_2^2 33b_1^2 \mathbf{44a_1^1} 16a_2^2 34b_1^2 17a_2^2 45a_1^2 18a_2^2 24b_2^2\}$	3.82
		$^2B_1$, $\{\ldots 15a_2^2 21b_2^2 31b_1^2 41a_1^2 42a_1^2 22b_2^2 32b_1^2 43a_1^2 23b_2^2 \mathbf{33b_1^1} 44a_1^2 16a_2^2 34b_1^2 17a_2^2 45a_1^2 18a_2^2 24b_2^2\}$	3.98
C	4.08(6)	$^2B_2$, $\{\ldots 15a_2^2 21b_2^2 31b_1^2 41a_1^2 42a_1^2 22b_2^2 32b_1^2 43a_1^2 \mathbf{23b_2^1} 33b_1^2 44a_1^2 16a_2^2 34b_1^2 17a_2^2 45a_1^2 18a_2^2 24b_2^2\}$	4.20
		$^2A_1$, $\{\ldots 15a_2^2 21b_2^2 31b_1^2 41a_1^2 42a_1^2 22b_2^2 32b_1^2 \mathbf{43a_1^1} 23b_2^2 33b_1^2 44a_1^2 16a_2^2 34b_1^2 17a_2^2 45a_1^2 18a_2^2 24b_2^2\}$	4.25
		$^2B_1$, $\{\ldots 15a_2^2 21b_2^2 31b_1^2 41a_1^2 42a_1^2 22b_2^2 \mathbf{32b_1^1} 43a_1^2 23b_2^2 33b_1^2 44a_1^2 16a_2^2 34b_1^2 17a_2^2 45a_1^2 18a_2^2 24b_2^2\}$	4.29
D	4.35(6)	$^2B_2$, $\{\ldots 15a_2^2 21b_2^2 31b_1^2 41a_1^2 42a_1^2 \mathbf{22b_2^1} 32b_1^2 43a_1^2 23b_2^2 33b_1^2 44a_1^2 16a_2^2 34b_1^2 17a_2^2 45a_1^2 18a_2^2 24b_2^2\}$	4.49
E	~ 5.04(5)	$^2A_1$, $\{\ldots 15a_2^2 21b_2^2 31b_1^2 41a_1^2 \mathbf{42a_1^1} 22b_2^2 32b_1^2 43a_1^2 23b_2^2 33b_1^2 44a_1^2 16a_2^2 34b_1^2 17a_2^2 45a_1^2 18a_2^2 24b_2^2\}$	5.00
F	~ 5.27(4)	$^2A_1$, $\{\ldots 15a_2^2 21b_2^2 31b_1^2 \mathbf{41a_1^1} 42a_1^2 22b_2^2 32b_1^2 43a_1^2 23b_2^2 33b_1^2 44a_1^2 16a_2^2 34b_1^2 17a_2^2 45a_1^2 18a_2^2 24b_2^2\}$	5.40
G	~ 5.55(5)	$^2B_1$, $\{\ldots 15a_2^2 21b_2^2 \mathbf{31b_1^1} 41a_1^2 42a_1^2 22b_2^2 32b_1^2 43a_1^2 23b_2^2 33b_1^2 44a_1^2 16a_2^2 34b_1^2 17a_2^2 45a_1^2 18a_2^2 24b_2^2\}$	5.68
H	~5.8	$^2B_2$, $\{\ldots 15a_2^2 \mathbf{21b_2^1} 31b_1^2 41a_1^2 42a_1^2 22b_2^2 32b_1^2 43a_1^2 23b_2^2 33b_1^2 44a_1^2 16a_2^2 34b_1^2 17a_2^2 45a_1^2 18a_2^2 24b_2^2\}$	6.51

Table S2: Cartesian coordinates of the C_{2v} ($^1A_1$) global minimum tilted inverse triple-decker structure of $La_3B_{14}^-$ at the PBE0/TZP level of theory.

1.B	-2.819237	-0.794873	1.561375
2.B	2.819237	-0.794873	1.561375
3.B	-2.097215	-1.878356	0.758391
4.B	-0.853293	1.897244	-0.243491
5.B	0.000000	0.887847	-1.230163
6.B	0.853293	-1.897244	-0.243491
7.B	0.000000	-0.887847	-1.230163
8.B	0.853293	1.897244	-0.243491
9.B	-2.097215	1.878356	0.758391
10.B	2.097215	1.878356	0.758391
11.B	-2.819237	0.794873	1.561375
12.B	2.819237	0.794873	1.561375
13.La	-2.554884	0.000000	-1.092416
14.La	0.000000	0.000000	1.738465
15.La	2.554884	0.000000	-1.092416
16.B	-0.853293	-1.897244	-0.243491
17.B	2.097215	-1.878356	0.758391

Table S3. Bond order indices from different approaches, density of electrons (ρ), energy density (E), Laplacian of electron density ($\nabla^2\rho$) and η index of different La-B and bridged B-B bonding at the PBE0/TZP level. The BCP and the corresponding paths are shown in the inserted figure.

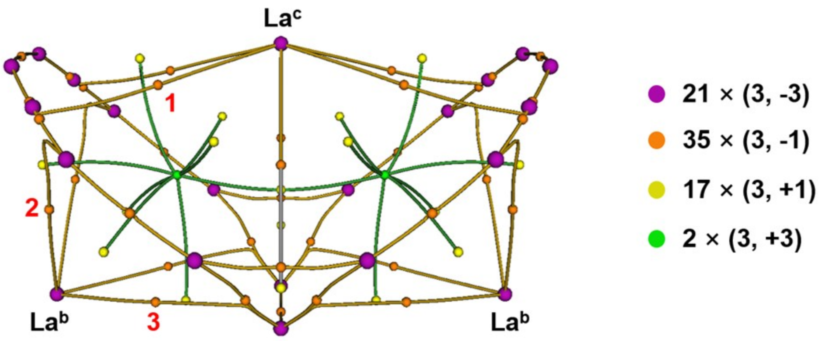

	Bond Order			ρ (r)	E (r)	$\nabla^2\rho$ (r)	η
	Mayer	**G-J**	**N-M (3)**				
La^c-B (1)	0.23	0.27	0.23	0.031	-0.0035	0.051	0.24
La^b-B (2)	0.39	0.36	0.39	0.048	-0.0092	0.068	0.28
La^b-B (3)	0.36	0.38	0.41	0.048	-0.0089	0.070	0.31
B-B bridge	0.78	0.75	0.82	0.139	-0.0933	-0.191	3.95

Table S4: Cartesian coordinates of the extended 1D lanthanide-boron nanostructures, C_{2v} ($^1A_1$) $La_5B_{26}^-$ and C_s ($^1A'$) $La_7B_{38}^-$ at the PBE/TZP level of theory (see Figure 5).

C_{2v} ($^1A_1$) $La_5B_{26}^-$:

1.B	0.778231	5.710435	-1.401119
2.B	1.849181	4.965130	-0.604843
3.B	-1.889049	3.741106	0.393252
4.B	-0.854586	2.869797	1.315278
5.B	1.848404	2.067315	0.301473
6.B	0.854586	2.869797	1.315278
7.B	-1.848404	2.067315	0.301473
8.B	-1.849181	4.965130	-0.604843
9.B	-1.850692	0.826933	-0.683590
10.B	-0.778231	5.710435	-1.401119
11.La	0.000000	5.409118	1.289767
12.La	0.000000	2.861323	-1.604438
13.B	1.889049	3.741106	0.393252
14.B	1.850692	0.826933	-0.683590
15.B	0.831290	0.000000	-1.648713
16.B	0.778231	-5.710435	-1.401119
17.B	1.850692	-0.826933	-0.683590
18.B	-1.848404	-2.067315	0.301473
19.B	-0.854586	-2.869797	1.315278
20.B	1.889049	-3.741106	0.393252
21.B	0.854586	-2.869797	1.315278
22.B	-1.889049	-3.741106	0.393252
23.B	-1.850692	-0.826933	-0.683590

24.B	-1.849181	-4.965130	-0.604843
25.B	-0.831290	0.000000	-1.648713
26.B	-0.778231	-5.710435	-1.401119
27.La	0.000000	0.000000	1.182715
28.La	0.000000	-2.861323	-1.604438
29.La	0.000000	-5.409118	1.289767
30.B	1.848404	-2.067315	0.301473
31.B	1.849181	-4.965130	-0.604843

C_s ($^1A'$) $La_7B_{38}^-$:

1.B	1.339834	0.752896	8.584218
2.B	0.523688	1.831415	7.872155
3.B	-0.481274	-1.906498	6.631125
4.B	-1.360113	-0.855603	5.769311
5.B	-0.325395	1.885363	4.996212
6.B	-1.349427	0.833355	5.747158
7.B	-0.315381	-1.848407	4.962886
8.B	0.529506	-1.876832	7.846493
9.B	0.607092	-1.840399	3.698037
10.B	1.338547	-0.803626	8.576689
11.La	-1.351000	-0.019085	8.301335
12.La	1.550800	-0.002875	5.760121
13.B	-0.483352	1.885620	6.649044
14.B	0.631296	1.879108	3.741948
15.B	1.599672	0.850627	2.933851
16.B	1.599672	0.850627	-2.933851
17.B	0.623718	1.874447	2.094262
18.B	-0.355313	-1.820074	0.845145
19.B	-1.351736	-0.872122	0.000000
20.B	-0.325027	1.817981	-0.830489
21.B	-1.288946	0.797652	0.000000
22.B	-0.355313	-1.820074	-0.845145
23.B	0.661801	-1.881887	2.062872
24.B	0.661801	-1.881887	-2.062872
25.B	1.572180	-0.784418	2.828364
26.B	1.572180	-0.784418	-2.828364
27.La	-1.256680	0.031234	2.847892
28.La	1.567617	-0.011547	0.000000
29.La	-1.256680	0.031234	-2.847892
30.B	-0.325027	1.817981	0.830489
31.B	0.623718	1.874447	-2.094262
32.B	1.339834	0.752896	-8.584218
33.B	0.631296	1.879108	-3.741948
34.B	-0.315381	-1.848407	-4.962886
35.B	-1.360113	-0.855603	-5.769311
36.B	-0.483352	1.885620	-6.649044
37.B	-1.349427	0.833355	-5.747158
38.B	-0.481274	-1.906498	-6.631125
39.B	0.607092	-1.840399	-3.698037
40.B	0.529506	-1.876832	-7.846493
41.B	1.338547	-0.803626	-8.576689
42.La	1.550800	-0.002875	-5.760121
43.La	-1.351000	-0.019085	-8.301335
44.B	-0.325395	1.885363	-4.996212
45.B	0.523688	1.831415	-7.872155